LETTER

doi:10.1038/nature24056

Network control principles predict neuron function in the *Caenorhabditis elegans* connectome

Gang Yan[1,2]*, Petra E. Vértes[3]*, Emma K. Towlson[1]*, Yee Lian Chew[4], Denise S. Walker[4], William R. Schafer[4] & Albert-László Barabási[1,5,6,7]

Recent studies on the controllability of complex systems offer a powerful mathematical framework to systematically explore the structure–function relationship in biological, social, and technological networks[1–3]. Despite theoretical advances, we lack direct experimental proof of the validity of these widely used control principles. Here we fill this gap by applying a control framework to the connectome of the nematode *Caenorhabditis elegans*[4–6], allowing us to predict the involvement of each *C. elegans* neuron in locomotor behaviours. We predict that control of the muscles or motor neurons requires 12 neuronal classes, which include neuronal groups previously implicated in locomotion by laser ablation[7–13], as well as one previously uncharacterized neuron, PDB. We validate this prediction experimentally, finding that the ablation of PDB leads to a significant loss of dorsoventral polarity in large body bends. Importantly, control principles also allow us to investigate the involvement of individual neurons within each neuronal class. For example, we predict that, within the class of DD motor neurons, only three (DD04, DD05, or DD06) should affect locomotion when ablated individually. This prediction is also confirmed; single cell ablations of DD04 or DD05 specifically affect posterior body movements, whereas ablations of DD02 or DD03 do not. Our predictions are robust to deletions of weak connections, missing connections, and rewired connections in the current connectome, indicating the potential applicability of this analytical framework to larger and less well-characterized connectomes.

Control theory probes a system's ability to drive its output towards a desired outcome through the application of suitable input signals to selected driver nodes[3]. With a connectome featuring well-defined input nodes, and experimentally testable behavioural responses acting as outputs, the nematode worm *C. elegans* provides an ideal test-bed for network control principles. For example, *C. elegans* responds to anterior (posterior) gentle body touch with backward (forward) locomotion. It senses touch via the sensory neurons ALM, AVM, and PLM, which serve as input nodes (Fig. 1a), processing this information through a network of 279 non-pharyngeal neurons connected by 2,194 directed synaptic connections and 1,028 reciprocal gap junctions. Of these, 124 motor neurons connect to 95 muscles via 552 neuromuscular junctions, inducing the experimentally observable locomotive patterns. So far, *C. elegans* is the only organism for which the wiring diagram of its complete nervous system has been mapped with reasonable accuracy at the cellular level[4–6]. Despite this structural information, which has been available for decades, it has proved difficult to systematically predict the functional involvement of specific neurons in defined behavioural responses.

From a network perspective, if the removal of a neuron physically disconnects one or more muscles from the input, its effect on locomotion is self-evident. Yet, given the dense wiring of the *C. elegans* connectome (Fig. 1c and Extended Data Fig. 1), no single neuron class ablation can disconnect the pathways between touch sensory receptors and muscles in the adult worm (see Supplementary Information section IIB). Consequently, straightforward connectivity analyses cannot reveal the involvement of individual neurons in locomotion. Prompted by this failure, we hypothesized that neurons whose absence alters the controllability of specific groups of muscles would lead to changes in locomotion patterns when ablated *in vivo*. We then applied network control principles to this connectome, expecting to reveal both neurons with known importance to locomotion and neurons whose involvement in locomotion was previously unknown, hence offering novel, experimentally testable predictions.

We model the nematode nervous system as a directed network whose nodes include neurons and muscles, and whose links represent the electrical and chemical synaptic connections between them, including neuromuscular junctions. Formally, the dynamics of the system composed of N neurons and M muscles is described by

$$\dot{\boldsymbol{z}}(t) = \boldsymbol{f}(\boldsymbol{z}, \boldsymbol{v}, t) \tag{1}$$

where $\boldsymbol{z}(t) = [z_1(t), z_2(t), \ldots, z_{N+M}(t)]^{\mathrm{T}}$ denotes the states of $N+M$ nodes at time t, $\boldsymbol{f}(*) = [f_1(*), f_2(*), \ldots, f_{N+M}(*)]^{\mathrm{T}}$ captures the nonlinear dynamics of each node, and $\boldsymbol{v}(t) = [v_1(t), v_2(t), \ldots, v_S(t)]^{\mathrm{T}}$ represents the external stimuli applied to the S touch receptor neurons. Assuming that in the absence of additional stimuli the nervous system is at a fixed point $\boldsymbol{z}^*$, where $\boldsymbol{f}(\boldsymbol{z}^*, \boldsymbol{v}^*, t) = 0$, and using $\boldsymbol{x}(t) = \boldsymbol{z}(t) - \boldsymbol{z}^*$ and $\boldsymbol{u}(t) = \boldsymbol{v}(t) - \boldsymbol{v}^*$, equation (1) can be linearized, obtaining

$$\begin{cases} \dot{\boldsymbol{x}}(t) = A\boldsymbol{x}(t) + B\boldsymbol{u}(t) \\ \boldsymbol{y}(t) = C\boldsymbol{x}(t), \end{cases} \tag{2}$$

where $A \equiv \frac{\partial \boldsymbol{f}}{\partial \boldsymbol{z}}\big|_{\boldsymbol{z}^*, \boldsymbol{v}^*}$ corresponds to the adjacency matrix of the connectome, with non-zero elements A_{ii} that represent the nodal dynamics of node i; the input matrix $B \equiv \frac{\partial \boldsymbol{f}}{\partial \boldsymbol{v}}\Big|_{\boldsymbol{z}^*, \boldsymbol{v}^*}$ represents the receptor neurons on which the external signals are imposed, for example, ALML/R and AVM for anterior gentle touch; and the vector $\boldsymbol{y}(t)$, selected by the output matrix C, represents the states of the M muscle cells. In other words, the response of *C. elegans* to external stimuli can be formalized as a target control problem[14], asking whether the inputs received by receptors in B can control the state of the muscles listed in C. The muscles are controllable if, with a suitable choice of inputs $\boldsymbol{u}(t)$, they can move in any desired manner, that is, $\boldsymbol{y}(t)$ can reach an arbitrary position of the M-dimensional state space[15]. The nonlinearity of system (1) must be considered if we want to find out how to control the muscles. Here, however, we ask which neurons are necessary for control, which can be

[1]Center for Complex Network Research and Department of Physics, Northeastern University, Boston, Massachusetts 02115, USA. [2]School of Physics Science and Engineering, Tongji University, Shanghai 200092, China. [3]Department of Psychiatry, Behavioural and Clinical Neuroscience Institute, University of Cambridge, Cambridge CB2 0SZ, UK. [4]Division of Neurobiology, MRC Laboratory of Molecular Biology, Cambridge Biomedical Campus, Francis Crick Avenue, Cambridge CB2 0QH, UK. [5]Center for Cancer Systems Biology, Dana Farber Cancer Institute, Boston, Massachusetts 02115, USA. [6]Department of Medicine, Brigham and Women's Hospital, Harvard Medical School, Boston, Massachusetts 02115, USA. [7]Center for Network Science, Central European University, H-1051 Budapest, Hungary.
*These authors contributed equally to this work.

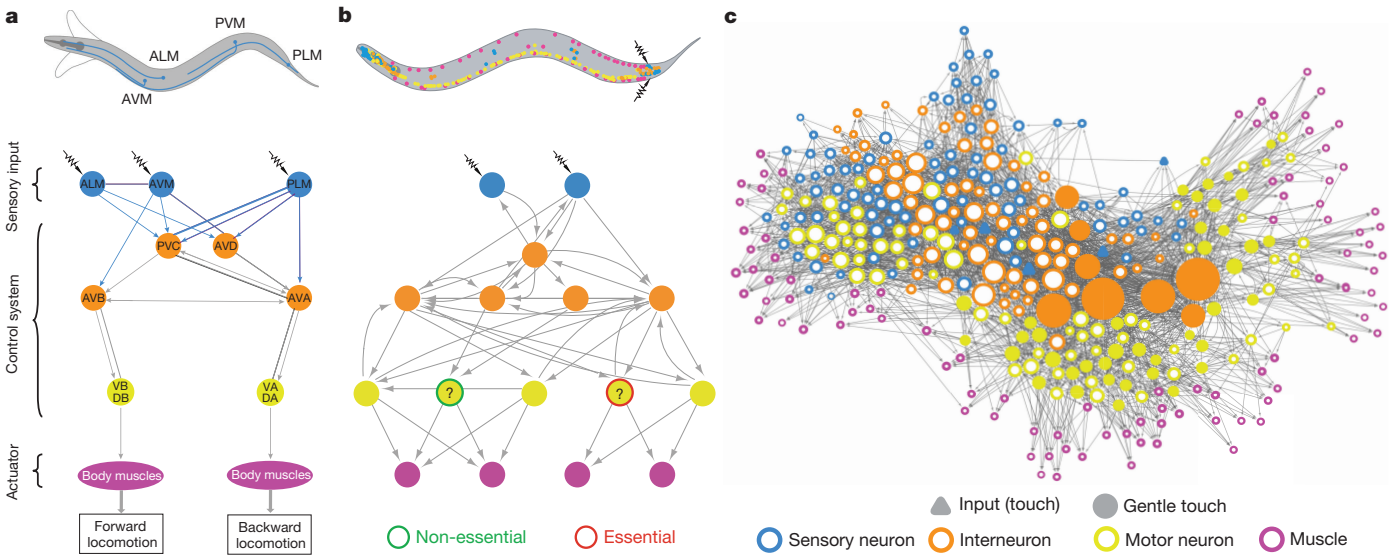

Figure 1 | Controlling the *C. elegans* neural network. a, Schematic neural circuit for locomotor response to gentle touch in *C. elegans* (adapted after ref. 30; see Supplementary Information section IIIA). **b**, Graphical representation of the proposed control framework. According to the principles illustrated in Fig. 2a–d, if removal of a neuron disrupts controllability of the muscles, we designate it 'essential' for locomotion; if not, we call it 'non-essential'. To make this assessment, we first mapped the *C. elegans* responsive locomotor behaviours into a target network control problem, asking to what degree the sensory neurons (blue) can control the muscles (pink). This allowed us to predict the previously unknown involvement of PDB in *C. elegans* locomotion, and functional differences between individual neurons within the DD neuronal class. **c**, The *C. elegans* connectome used in our study, consisting of 279 neurons (the 282 non-pharyngeal neurons, excluding CANL/R and VC06 which do not make connections with the rest of the network) and 95 muscles. Node size is proportional to the sum of its in- and out-degrees. Filled nodes represent the neurons traditionally assigned to the circuits responsible for gentle touch response, hinting at the complexity of predicting neuronal function from the wiring diagram alone.

captured by the controllability of the linearized system (2). Indeed, if the linearized system (2) is locally controllable along a specific trajectory in state space, then the original nonlinear system (1) is also controllable along the same trajectory[15]. Furthermore, linear controllability predictions are consistent with simulations of neuronal networks with nonlinear dynamics[16,17].

To understand how control considerations differ from simple connectivity-based predictions, consider Fig. 2a, exploring whether nodes 2 and 3 can be controlled by a signal applied to node 1. Topologically the system appears controllable, as the signal can reach all nodes. Yet, the classic Kalman condition[18] tells us that the responses of nodes 2 and 3 to this signal are always correlated, hence we cannot control them independently, making the system as a whole uncontrollable. To gain full control over all three nodes, we need to apply one additional control signal to node 2 or 3 (Fig. 2b). We encounter the same situation when m independent signals aim to control k nodes, a configuration that is controllable only if $m \geq k$ (Fig. 2c, d). In a similar spirit, we derive the criterion for muscle controllability and apply it to analyse the *C. elegans* nervous system (Supplementary Information section IIB and Extended Data Fig. 2).

Here, we applied this network control framework to predict which neurons are critical in the response to gentle touch, in the sense that their removal (ablation) would decrease the number of controllable muscles. We found that even in the intact worm, only 89 of the 95 muscles are independently controllable. We then explored the impact of ablating each of the 103 neuronal classes (see Supplementary Information section IB for neuron classification) individually. We found that the removal of the vast majority of neuron classes had no impact on muscle controllability. Our initial analysis did identify, however, nine classes predicted to affect muscle control: the seven major classes of motor neurons (DA, DB, DD, VA, VB, VD, and AS), and the premotor interneuron AVA (Table 1; see also Extended Data Figs 3–5). Each of these classes has been previously implicated, through genetic, neuroimaging, optogenetic, and cell ablation experiments, in the direct control of the body neuromusculature (see Supplementary Information section IIIA).

Interestingly, the control analysis also predicted locomotor defects following the ablation of a ninth neuron, PDB, not previously implicated in locomotion. As shown in Fig. 2e, while PDB directly connects to muscles MVR21 and MVL22, it apparently plays no key topological role as in its absence the signal transmitted by the receptor neurons for anterior gentle touch, AVM and ALML/R, can still reach all muscles. However, from a control perspective, we expect that the ablation of PDB should affect worm locomotion (see Fig. 2e for a full explanation). Since ablation experiments for PDB have not previously been reported, this prediction offers the first direct, falsifiable experimental test of the network control framework.

Most existing results on neuron ablation remove all members of a neuron class simultaneously[7,10–12], but control principles can go further, predicting which of the individual neurons are responsible for the loss of control. To show this we applied the linearized system (2) to each individual neuron within the DD class. Intriguingly, we found that the individual ablation of DD01, DD02, or DD03 did not alter the controllability of the muscles, but DD04, DD05, and DD06 did (Fig. 3a). This result was unexpected, because the general pattern of connectivity is thought to be similar among the DD class. Nevertheless, we predict that the individual ablation of DD04, DD05, or DD06 should be sufficient to impair *C. elegans* locomotion, offering a second set of specific, unanticipated, and falsifiable predictions, now regarding the functional differences between individual neurons within a class.

To test the validity of our two sets of predictions, we performed laser ablation of individual neurons[9] and analysed the spontaneous locomotor behaviour of freely moving worms on food (see https://doi.org/10.6084/m9.figshare.c.3796345 for complete data[19]). We used an automated tracking system[20] to compare the locomotion pattern of PDB- and DD-ablated animals with mock-ablated worms, focusing on four fundamental components of worm body morphology known as eigenworms, which provide a low-dimensional but relatively complete description of *C. elegans* body postures[21]. Under our recording conditions, the first Eigen projection represents a large body bend, the second and third represent components of the sinusoidal travelling wave that drives crawling movement, and the fourth represents small movements at the head and tail[22].

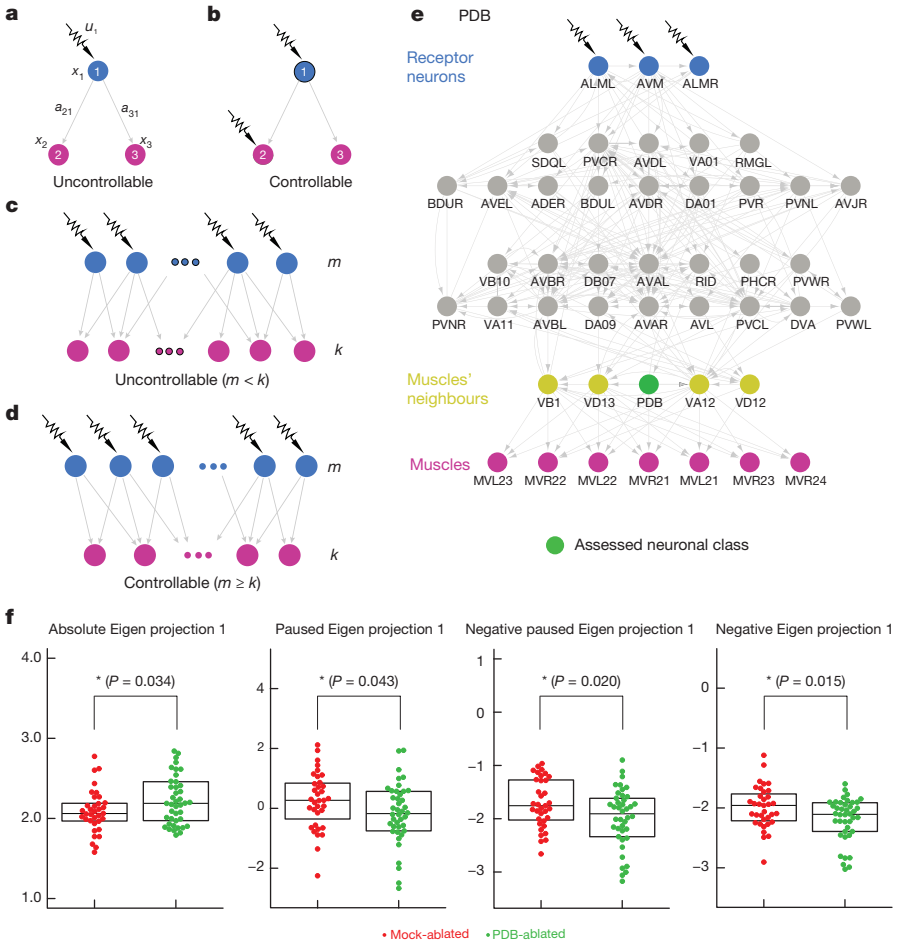

Figure 2 | Novel prediction and experimental confirmation of PDB involvement in locomotion. a, According to control theory, nodes 2 and 3 (pink) cannot be controlled by a single signal $u_1(t)$. By equation (2), the time evolution of $x_2(t)$ and $x_3(t)$ follows $a_{31}\dot{x}_2(t) = a_{21}\dot{x}_3(t)$, hence no signal $u_1(t)$ is able to control $x_2(t)$ and $x_3(t)$ independently of each other. To independently control nodes 2 and 3, we need two input signals, as shown in **b**. Similarly, when m independent signals aim to control k nodes connected to them, as shown in **c**, the pink nodes are not controllable unless $m \geq k$, which is the case shown in **d**. **e**, To explore the control role of PDB, we show the shortest paths through which control signals can pass from receptor neurons (blue) to downstream muscles (pink). Control analysis finds that the five motor neurons, {VB11, VD13, PDB, VA12, VD12}, receive independent signals from {ALML, ALMR, AVM} (see Supplementary Information section IIB). According to the principle illustrated in **c**, in the intact worm, five of the seven muscles are independently controllable. When PDB is ablated, control signals can still reach all seven muscles, but the ablation of PDB forces the signal through only four neurons, reducing the number of independently controllable muscles from five to four. **f**, Experimental validation of the involvement of PDB in locomotion. $N = 43$ PDB ablations were tested in the same experiment together with $n = 35$ mock-ablated controls. Error bars, mean ± s.d. Ablation of PDB resulted in significant abnormalities in Eigen projection 1 features and a loss of ventral bias to deep body bends (Supplementary Table 3). Statistical test: multiple t-tests, significance level = 0.05. See Supplementary Information section IIIB for experimental details of laser ablations, subsequent data analysis, and exact P values.

We first tested the effect of ablating the PDB neuron on locomotion. We observed that PDB-ablated animals showed significant and reproducible abnormalities in parameters related to the first Eigen projection (EP1; Fig. 2f, Supplementary Table 2 and Extended Data Fig. 6a) compared with mock-ablated animals of the same genotype. Specifically, ablated animals showed a higher incidence of highly negative EP1 values, which correlate with deep bends on the dorsal side of the body. Since large bends, or omega turns, are strongly biased to the ventral side in normal worms[23,24], this suggested a loss of ventral bias in PDB-ablated animals. Indeed, we observed that PDB-ablated animals showed a significantly lower frequency of ventral omega turns (63.8% versus 81.9% for control; $n > 125$, $P < 0.0005$ by two-tailed z-test; see Supplementary Table 3) compared with mock-ablated animals. These results are consistent with our prediction that PDB is essential for the control of the body neuromusculature.

We next tested the effects of ablating individual DD neurons on locomotor control. As predicted, ablations of DD02 showed no significant abnormalities in locomotion compared with mock-ablated animals. In contrast, we found that DD05-ablated worms showed significantly lower absolute values for the fourth eigenworm (EP4) during forward movement (Fig. 3b, c, Supplementary Table 1 and Extended Data Fig. 6b), correlating with a reduction in tail movement during forward locomotion. A similar effect on EP4 parameters was observed

Table 1 | Neuronal predictions

Control	Predicted neuron classes	Experimental facts
Control muscles	DA, DB	Loss of backward/forward locomotion
	DD	Uncoordinated motion
	AVA	Uncoordinated motion
	VA, VB, VD, AS	Likely loss of locomotion
	PDB	**Verified by new experiments**
Control motor neurons	AVA, AVB	Uncoordinated motion
	AVD	Loss of reversal response
	PVC	Loss of reversal response

The 12 neuron classes predicted by control theoretic tools to be effective in locomotion and the known experimental results for ablation in adult *C. elegans*[10–13]. Highlighted in bold type is PDB, not previously associated with locomotion.

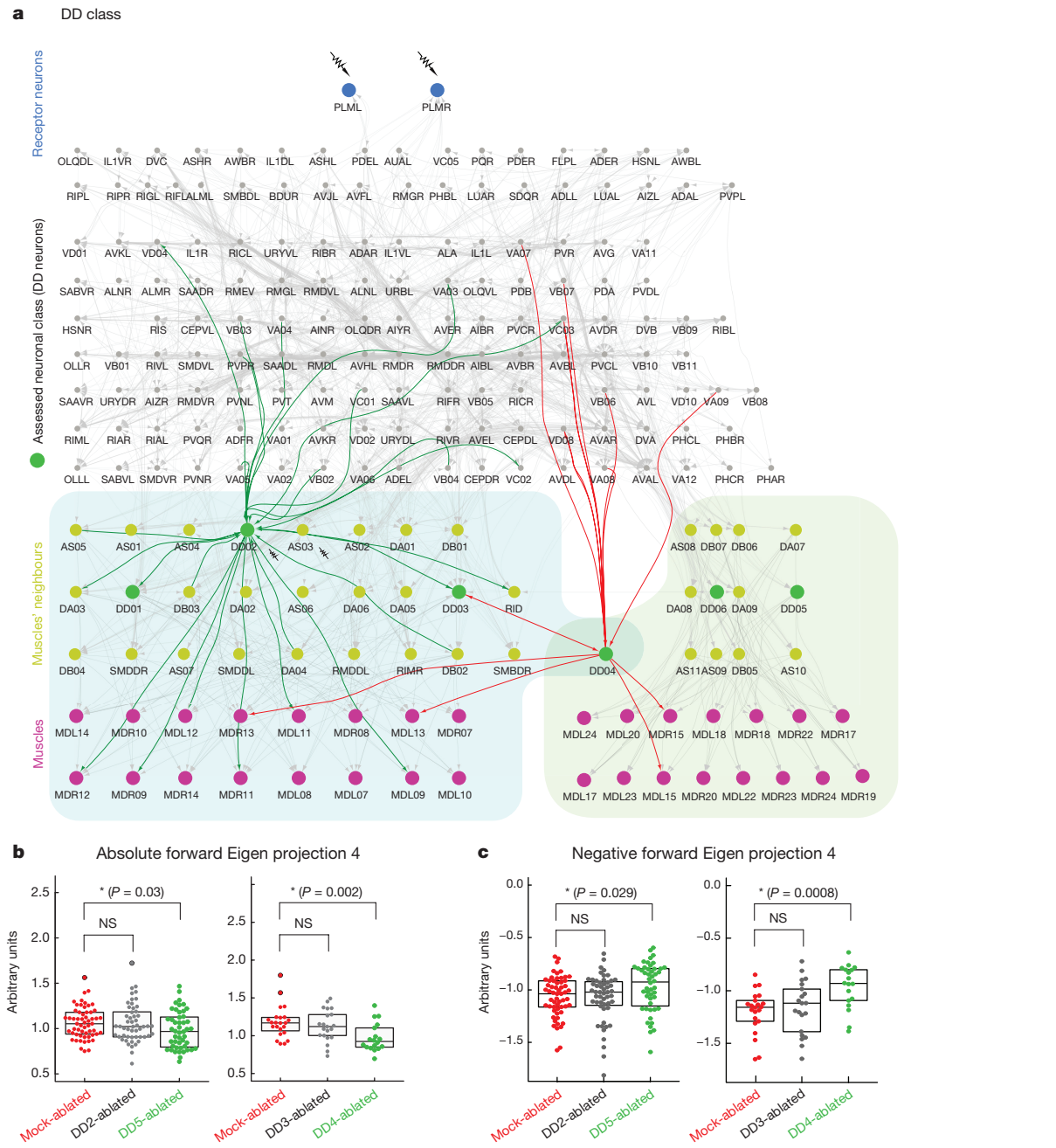

Figure 3 | Novel prediction and experimental confirmation for the effect of individual DD neurons on locomotion. a, To explore the control role of the DD neuronal class, comprising six neurons (DD01–DD06), we show the shortest paths through which control signals can pass from the receptor neurons to the 31 muscles. Right bottom corner (yellow highlight): in the intact adult, the 13 motor neurons that directly connect to the 15 muscles receive independent signals from PLML/R (see Supplementary Information section IIB). Hence, according to the control principle of Fig. 2c, 13 of the 15 muscles are independently controllable. When DD04, DD05, or DD06 is ablated, the number of controllable muscles decreases to 12, suggesting that DD04, DD05, and DD06 are individually indispensable for locomotion. Left bottom corner (blue highlight): control signals to the 16 muscles go through 27 neurons. When DD01, DD02, or DD03 is ablated, according to the principle in Fig. 2d the 26 remaining neurons are still able to independently control all 16 muscles, predicting that DD01, DD02, and DD03 are individually inessential for locomotion. The incoming and outgoing links of DD02 and DD04 are highlighted in green and red, respectively, as examples of the connectivity profiles of neurons from each group. **b**, **c**, Experimental validation. Individual ablation of DD04 or DD05, but not DD02 or DD03, affected the worm posture as indicated by statistically different Eigen projection 4 features. DD02 ($n = 52$) and DD05 ($n = 48$) ablations were tested in the same experiment together with mock-ablated controls ($n = 58$). DD03 ($n = 21$) and DD04 ($n = 18$) ablations were tested together in a separate experiment with new mock-ablated controls ($n = 23$). Error bars, mean ± s.d. Statistical test: multiple t-tests, significance level = 0.05; NS, not significant.

for DD04- but not DD03-ablated worms, consistent with DD04 and DD05 specifically affecting control of posterior body muscles. Taken together, the results of the PDB and DD ablations support our starting hypothesis that control principles can accurately identify individual neurons with key roles in the coordination of locomotion.

Motor neurons, which directly connect to muscle cells, play a unique role in transmitting motor commands to muscles. Our previous analysis focused on muscle control, allowing the motor neurons to be in arbitrary dynamical states, some of which may not be biologically realistic. We therefore refined our analysis to identify neurons required

to preserve the controllability of motor neurons. This control analysis predicts that AVB, AVD, and PVC are also crucial for locomotion (see Supplementary Information section IIB); the ablation of these neurons has been shown previously to profoundly disrupt forward movement[7,8,10] or the response to gentle touch[7] (Table 1). Thus, using motor neurons as targets for controllability led to a more complete set of predictions for the analysis of locomotor control.

The accuracy of the *C. elegans* connectome data is affected by several factors including human errors during mapping and synapse identification and the small number of animals reconstructed (only two), prompting us to explore the robustness of our predictions. Extended Data Fig. 7 shows the probability that a given neuron class, predicted to be essential for locomotion on the basis of the current data set, remains essential after randomly deleting weak links, adding links, and rewiring the existing links between neurons (see Supplementary Information section IVA for details). We find that the predictions for PDB, DA, DB, DD, VA, VB, VD, and AS are robust, remaining significant as we progressively alter as many as 100 links between neurons. The least robust prediction is for AVA, whose probability of being involved in control decreases with link addition/rewiring.

In summary, our ability to predict the importance of individual neurons in *C. elegans* locomotion shows that control principles offer a novel way to unveil how the connectome structure affects its function (see Fig. 1b and Extended Data Figs 8–10). In doing so, we provide the first experimental evidence for the relevance of control principles to the properties of real-world complex systems.

Our results raise several open questions and opportunities for future work. For example, the control principles of two distinct behaviours described by the same sets of input and output nodes cannot be distinguished on the basis of the connectome alone. However, if accurate link weights or activity patterns can be experimentally determined, the control framework can predict control energy and control time[25,26] and ultimately tease apart involvement of network components when the input and output nodes are indistinguishable. It is also theoretically possible to adapt our tools to temporally varying sensory inputs and behavioural responses invoking a framework to control temporal networks[27–29]. Finally, since meaningful predictions can be made despite some degree of uncertainty or incompleteness on the underlying connectome, we expect that the control framework introduced here is applicable to other neural wiring diagrams. Consequently, advances in mapping the *Drosophila* brain and other larger connectomes will yield unprecedented opportunities for deepening our understanding of both control principles and the mechanisms driving the function and activity of nervous systems.

Online Content Methods, along with any additional Extended Data display items and Source Data, are available in the online version of the paper; references unique to these sections appear only in the online paper.

Code Availability The code written for and used in this study is available from the corresponding author upon reasonable request.

Data Availability The experimental data generated and analysed during this study can be found at https://doi.org/10.6084/m9.figshare.c.3796345 (ref. 19).

Received 8 December 2016; accepted 4 September 2017.
Published online 18 October 2017.

1. Caldarelli, G. *Scale-Free Networks: Complex Webs in Nature and Technology* (Oxford Univ. Press, 2007).
2. Cohen, R. & Havlin, S. *Complex Networks: Structure, Robustness and Function* (Cambridge Univ. Press, 2010).
3. Liu, Y.-Y. & Barabási, A.-L. Control principles of complex networks. *Rev. Mod. Phys.* **88,** 035006 (2016).
4. White, J. G., Southgate, E., Thomson, J. N. & Brenner, S. The structure of the nervous system of the nematode *Caenorhabditis elegans*. *Phil. Trans. R. Soc. Lond. B* **314,** 1–340 (1986).
5. Chen, B. L. J. *Neuronal Network of C. elegans: From Anatomy to Behavior*. PhD thesis, Cold Spring Harbor Laboratory (2007).
6. Varshney, L. R., Chen, B. L., Paniagua, E., Hall, D. H. & Chklovskii, D. B. Structural properties of the *Caenorhabditis elegans* neuronal network. *PLoS Comput. Biol.* **7,** e1001066 (2011).
7. Chalfie, M. *et al.* The neural circuit for touch sensitivity in *Caenorhabditis elegans*. *J. Neurosci.* **5,** 956–964 (1985).
8. Zhen, M. & Samuel, A. D. *C. elegans* locomotion: small circuits, complex functions. *Curr. Opin. Neurobiol.* **33,** 117–126 (2015).
9. Bargmann, C. I. & Avery, L. Laser killing of cells in *Caenorhabditis elegans*. *Methods Cell Biol.* **48,** 225–250 (1995).
10. Wicks, S. R. & Rankin, C. H. Integration of mechanosensory stimuli in *Caenorhabditis elegans*. *J. Neurosci.* **15,** 2434–2444 (1995).
11. Tsalik, E. L. & Hobert, O. Functional mapping of neurons that control locomotory behavior in *Caenorhabditis elegans*. *J. Neurobiol.* **56,** 178–197 (2003).
12. Wakabayashi, T., Kitagawa, I. & Shingai, R. Neurons regulating the duration of forward locomotion in *Caenorhabditis elegans*. *Neurosci. Res.* **50,** 103–111 (2004).
13. Haspel, G., O'Donovan, M. J. & Hart, A. C. Motoneurons dedicated to either forward or backward locomotion in the nematode *Caenorhabditis elegans*. *J. Neurosci.* **30,** 11151–11156 (2010).
14. Gao, J., Liu, Y.-Y., D'Souza, R. M. & Barabási, A.-L. Target control of complex networks. *Nat. Commun.* **5,** 5415 (2014).
15. Coron, J.-M. *Control and Nonlinearity* (American Mathematical Society, 2009).
16. Whalen, A. J., Brennan, S. N., Sauer, T. D. & Schiff, S. J. Observability and controllability of nonlinear networks: the role of symmetry. *Phys. Rev. X* **5,** 011005 (2015).
17. Muldoon, S. F. *et al.* Stimulation-based control of dynamic brain networks. *PLoS Comput. Biol.* **12,** e1005076 (2016).
18. Kalman, R. E. Mathematical description of linear dynamical systems. *J. Soc. Indus. Appl. Math. A* **1,** 152–192 (1963).
19. Chew, Y. L. *et al.* Recordings of *Caenorhabditis elegans* locomotor behaviour following targeted ablation of single motorneurons. *Sci. Data* **4,** 170156 (2017).
20. Yemini, E., Jucikas, T., Grundy, L. J., Brown, A. E. & Schafer, W. R. A database of *Caenorhabditis elegans* behavioral phenotypes. *Nat. Methods* **10,** 877–879 (2013).
21. Stephens, G. J., Johnson-Kerner, B., Bialek, W. & Ryu, W. S. Dimensionality and dynamics in the behavior of *C. elegans*. *PLoS Comput. Biol.* **4,** e1000028 (2008).
22. Brown, A. E., Yemini, E. I., Grundy, L. J., Jucikas, T. & Schafer, W. R. A dictionary of behavioral motifs reveals clusters of genes affecting *Caenorhabditis elegans* locomotion. *Proc. Natl Acad. Sci. USA* **110,** 791–796 (2013).
23. Gray, J. M., Hill, J. J. & Bargmann, C. I. A circuit for navigation in *Caenorhabditis elegans*. *Proc. Natl Acad. Sci. USA* **102,** 3184–3191 (2005).
24. Huang, K. M., Cosman, P. & Schafer, W. R. Machine vision based detection of omega bends and reversals in *C. elegans*. *J. Neurosci. Methods* **158,** 323–336 (2006).
25. Yan, G. *et al.* Spectrum of controlling and observing complex networks. *Nat. Phys.* **11,** 779–786 (2015).
26. Gu, S. *et al.* Controllability of structural brain networks. *Nat. Commun.* **6,** 8414 (2015).
27. Pósfai, M. & Hövel, P. Structural controllability of temporal networks. *New J. Phys.* **16,** 123055 (2014).
28. Pan, Y. & Li, X. Structural controllability and controlling centrality of temporal networks. *PLoS ONE* **9,** e94998 (2014).
29. Li, A., Cornelius, S. P., Liu, Y. Y., Wang, L. & Barabási, A. L. The fundamental advantages of temporal networks. *arXiv*, 1607.06168 (2016).
30. Driscoll, M. & Kaplan, J. in *C. elegans II* (Cold Spring Harbor monograph series 33) (eds Riddle, D. L. *et al.*) Ch. 23 (Cold Spring Harbor Laboratory Press, 1997).

Supplementary Information is available in the online version of the paper.

Acknowledgements We thank M. Angulo, J. Gao, Y.-Y. Liu, J.-J. Slotine, K. Albrecht, S. P. Cornelius, and A. Li for discussions, and L. Grundy, A. Brown, and E. Yemini for help with analysis of tracking data. We are grateful to V. Butler and the Caenorhabditis Genetics Center, which is funded by National Institutes of Health Office of Research Infrastructure Programs (P40 OD010440), for *C. elegans* strains. This work is supported by the John Templeton Foundation: Mathematical and Physical Sciences grant number PFI-777; European Commission grant number 641191 (CIMPLEX); Medical Research Council grant number MC-A023-5PB91; Wellcome Trust grant number WT103784MA. P.E.V. is supported by the Medical Research Council grant number MR/K020706/1. Y.L.C. is supported by an EMBO Long Term Fellowship.

Author Contributions A.-L.B., G.Y., and P.E.V. conceived the project. G.Y. did the control analysis. P.E.V. and E.K.T. analysed the results. W.R.S. conceived the experimental validation. Y.L.C. and D.S.W. planned and performed the new experiments. Y.L.C. and W.R.S. analysed the experimental data, and W.R.S. and A.-L.B. discussed the results. A.-L.B., E.K.T., W.R.S., P.E.V., and G.Y. wrote the manuscript, Y.L.C. and D.S.W. edited it. G.Y., Y.L.C., and D.S.W. wrote the Supplementary Information, and W.R.S., E.K.T., and P.E.V. edited it.

Author Information Reprints and permissions information is available at www.nature.com/reprints. The authors declare no competing financial interests. Readers are welcome to comment on the online version of the paper. Publisher's note: Springer Nature remains neutral with regard to jurisdictional claims in published maps and institutional affiliations. Correspondence and requests for materials should be addressed to A.-L.B. (alb@neu.edu).

Reviewer Information *Nature* thanks C. Bargmann, E. Izquierdo and M. Zhen for their contribution to the peer review of this work.

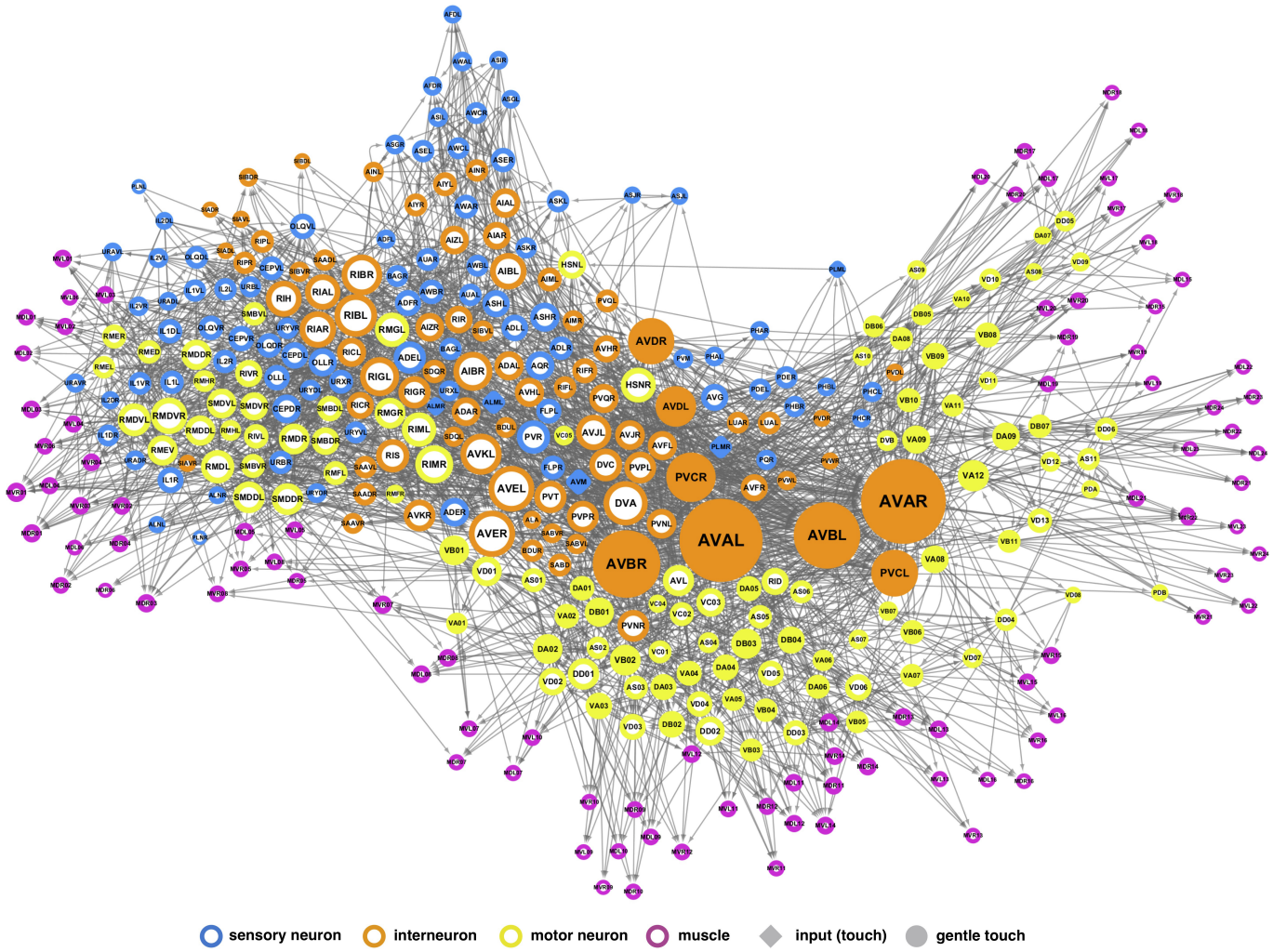

Extended Data Figure 1 | *C. elegans* connectome. The filled nodes are the previously known neurons involved in the worm's response to gentle touch.

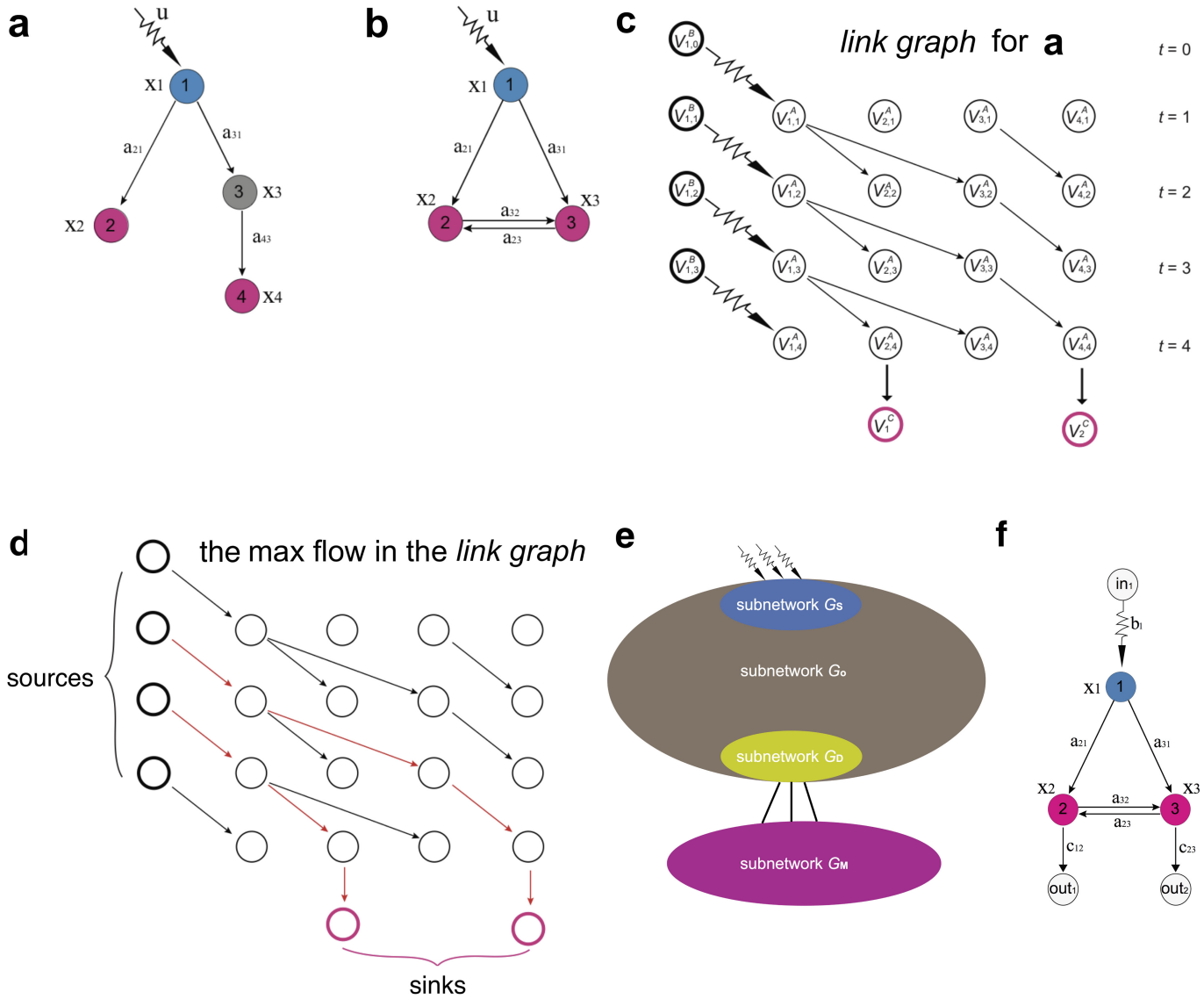

Extended Data Figure 2 | Structural controllability, the construction of the linking graph, and the derivation of the controllability criterion. **a**, **b**, The blue nodes receive external signals and the pink nodes are those we aim to control. Thus, $S=1$ and $M=2$ for both networks. **c**, The construction of the linking graph for the network in **a**. **d**, The calculation of the linking size can be mapped into a multi-source-multi-sink max-flow problem, with the constraint that the capacity of each node and each edge is one. The red edges show the two disjoint paths that achieve the maximum flow. **e**, **f**, Schematic picture for the derivation of the lower bound z_*.

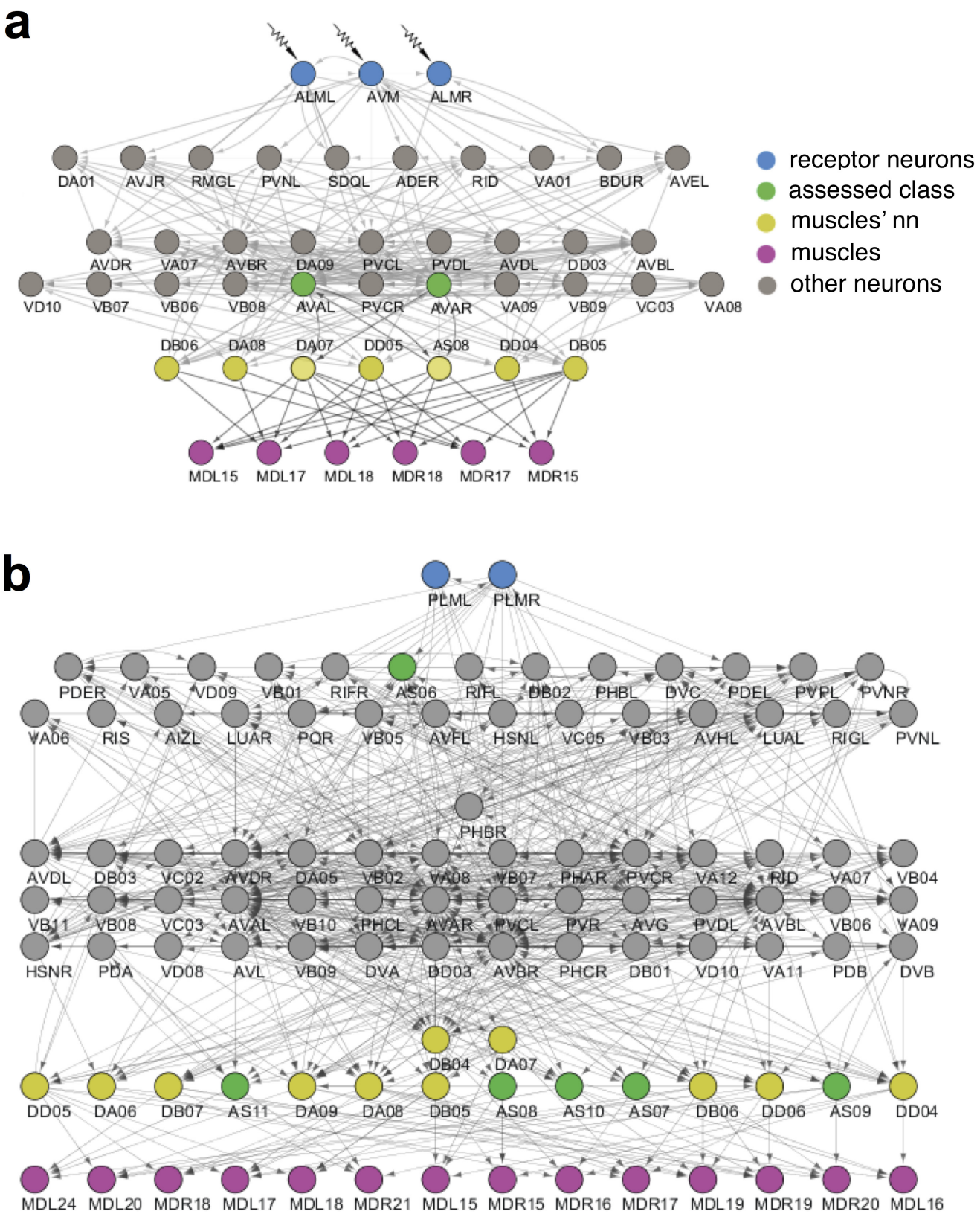

Extended Data Figure 3 | Control theoretic mechanisms of the loss of muscular control. Loss of control induced by the ablation of the AVA (**a**) or AS (**b**) neuronal class in *C. elegans*.

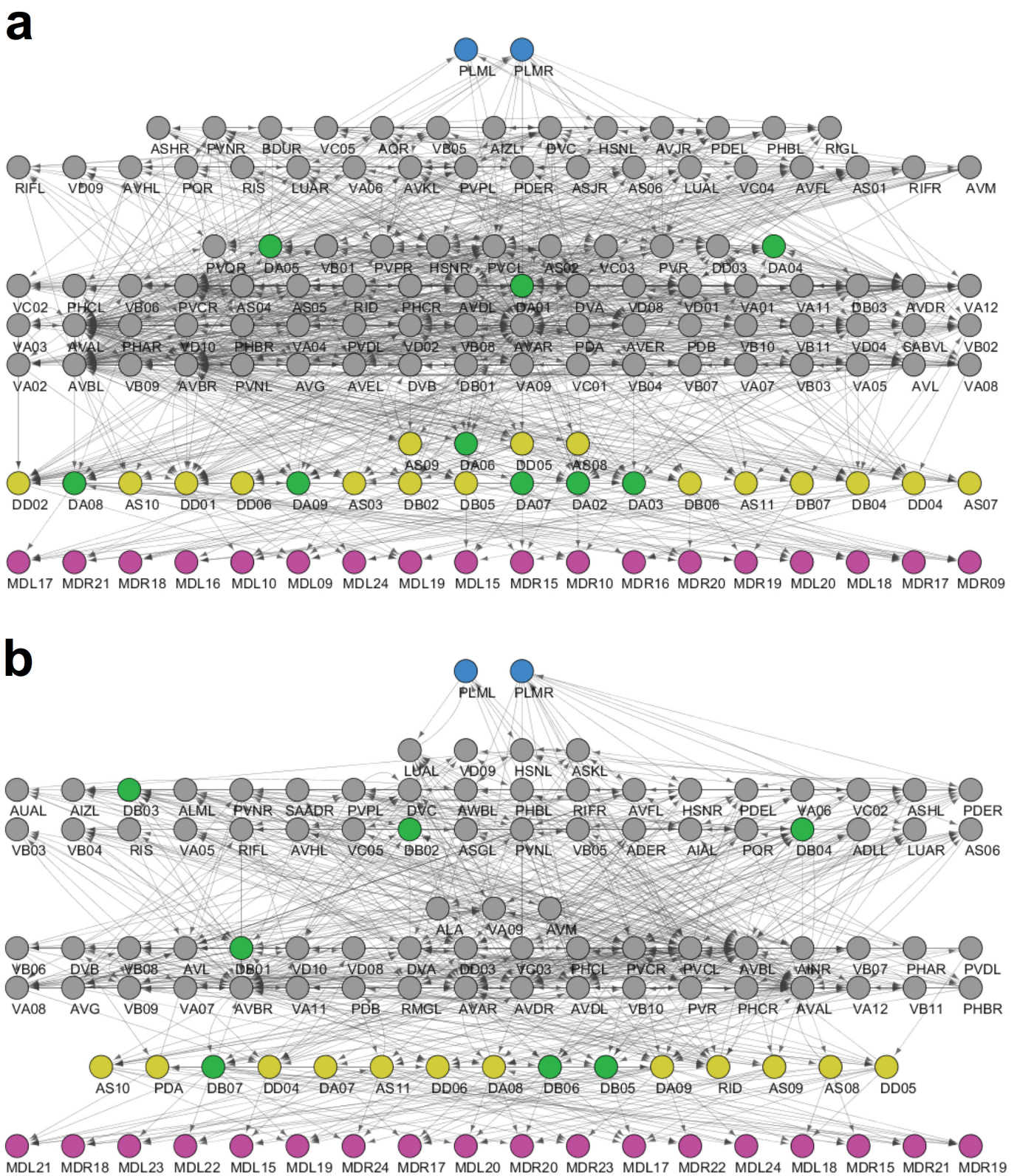

Extended Data Figure 4 | Control theoretic mechanisms of the loss of muscular control. Loss of control induced by the ablation of the DA (**a**) or DB (**b**) neuronal class in *C. elegans*.

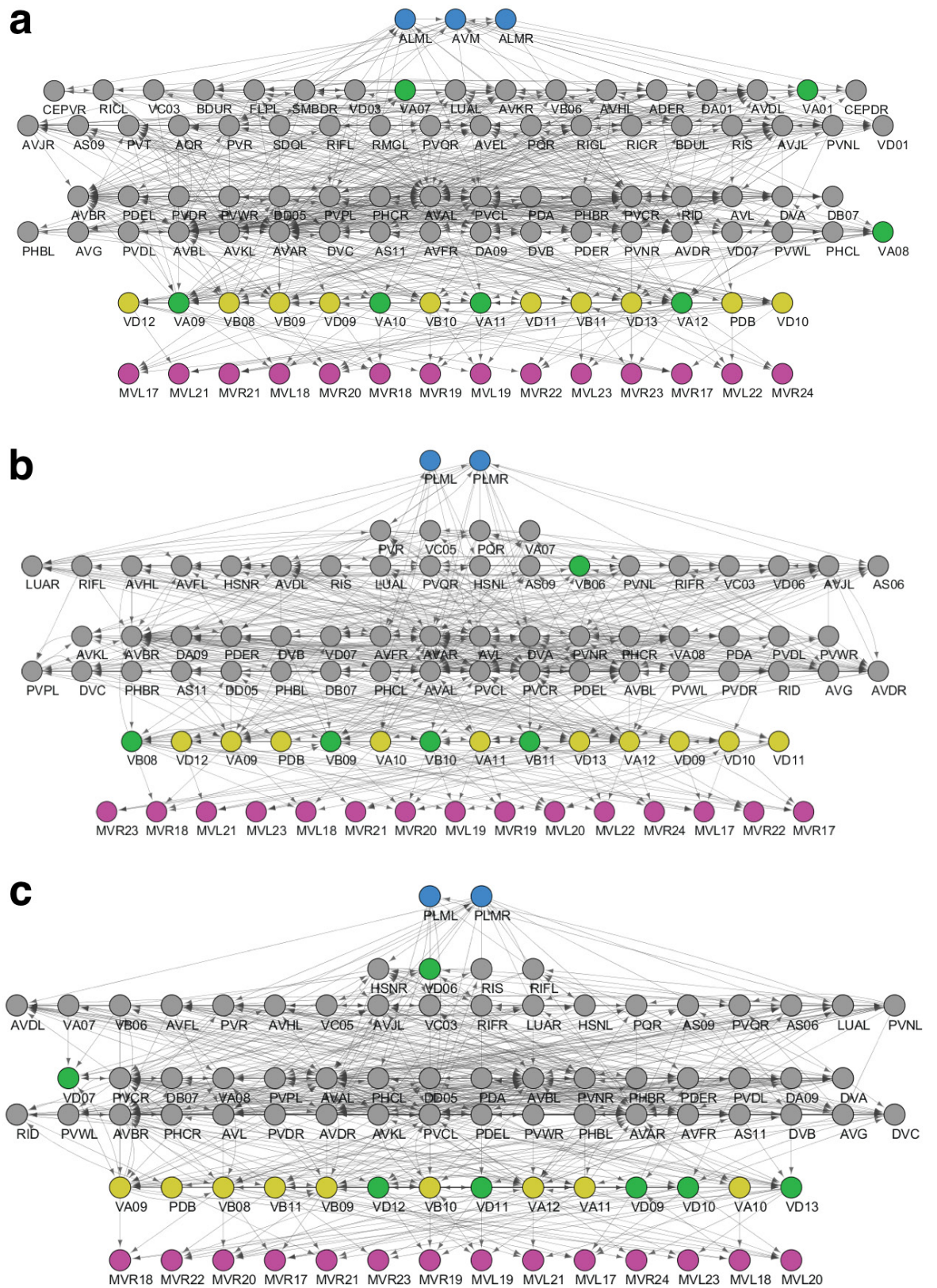

Extended Data Figure 5 | Control theoretic mechanisms of the loss of muscular control. Loss of control induced by the ablation of the VA (**a**), VB (**b**), or VD (**c**) neuronal class in *C. elegans*.

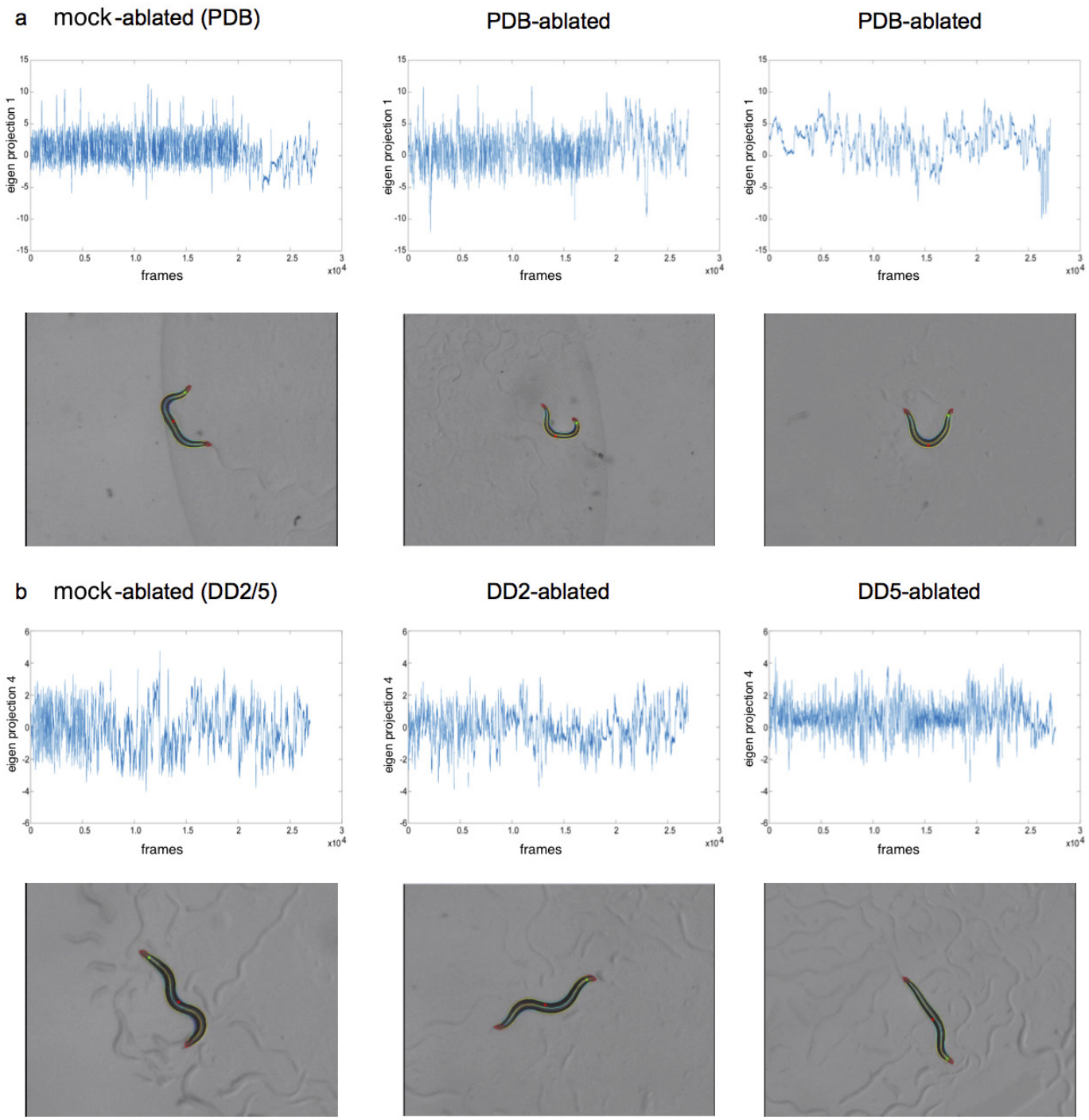

Extended Data Figure 6 | Illustrative examples of the behavioural phenotypes observed for PDB- and DD-ablated animals. Time series plots of sample videos, and still images from these videos, illustrating the locomotion abnormalities resulting from ablation. The green dot indicates the animal's head, and the red dot in the mid-body indicates the ventral side. **a**, For PDB-ablated animals compared with mock-ablated controls, we observed differences in Eigen projection 1, which describes the large wavelength body bends that occur during turning. The lower negative values observed in PDB ablations indicate a loss of the ventral bias to these turns. Still images show PDB-ablated animals making a large dorsal turn, whereas turns in control animals are usually ventral. The videos used here (from left to right) are 'mockPDB_onfood_L_2016_ 11_03__14_16_37___7___1', 'ablPDB_onfood_L_2016_11_03__14_40_04___4__2', and 'ablPDB_onfood_L_2016_11_04__14_28_26___5___1'. **b**, DD5-ablated animals showed lower values for Eigen projection 4, which captures the small wavelength oscillations in the head and tail. The lower values indicate a reduction in amplitude of tail oscillations compared with controls, that is, a characteristic stiff tail appearance. The videos shown here (from left to right) are 'mockDD_onfood_L_2016_10_29__13_13_35 ___7___6', 'DD2_onfood_R_2016_10_30__12_13_57___7___4', and 'DD5_onfood_L_2016_10_29__13_13_25___5___6'.

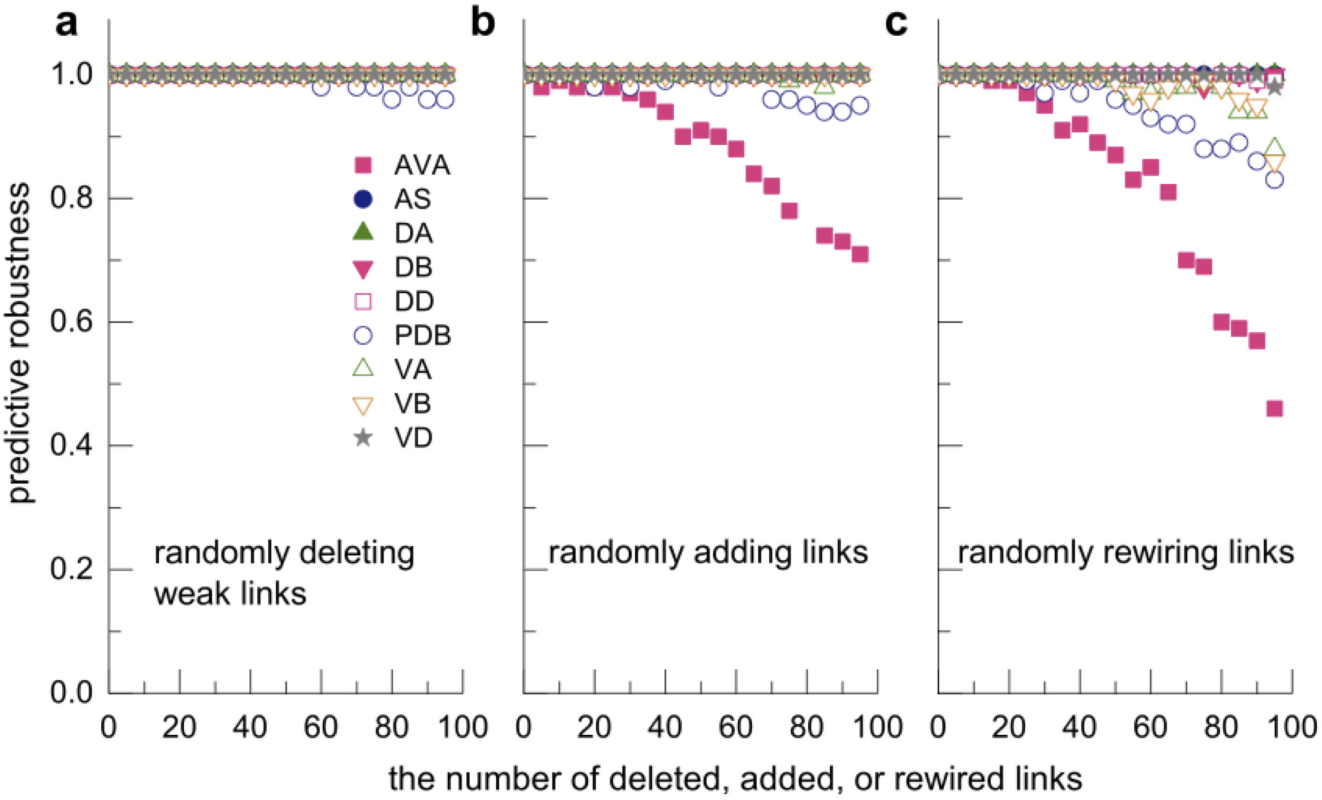

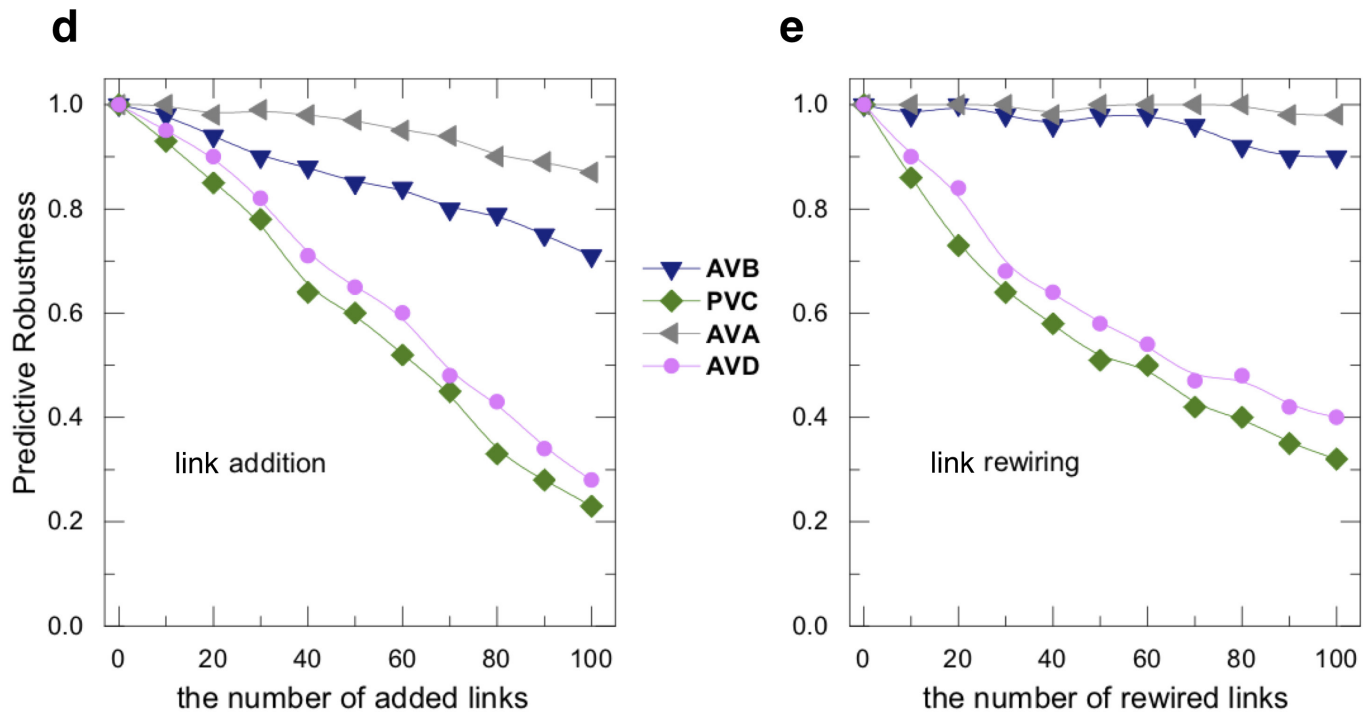

Extended Data Figure 7 | Predictive robustness against random deletions, additions, and rewiring of links. The vertical axis represents the probability that each of the predicted neuron classes remains significant in the controllability of muscles (**a**–**c**) or motor neurons (**d**, **e**) after the network is altered. The horizontal axis denotes the number of deleted weak links, added links, or rewired links between neurons in *C. elegans* connectome. Each probability is calculated from 200 independent runs.

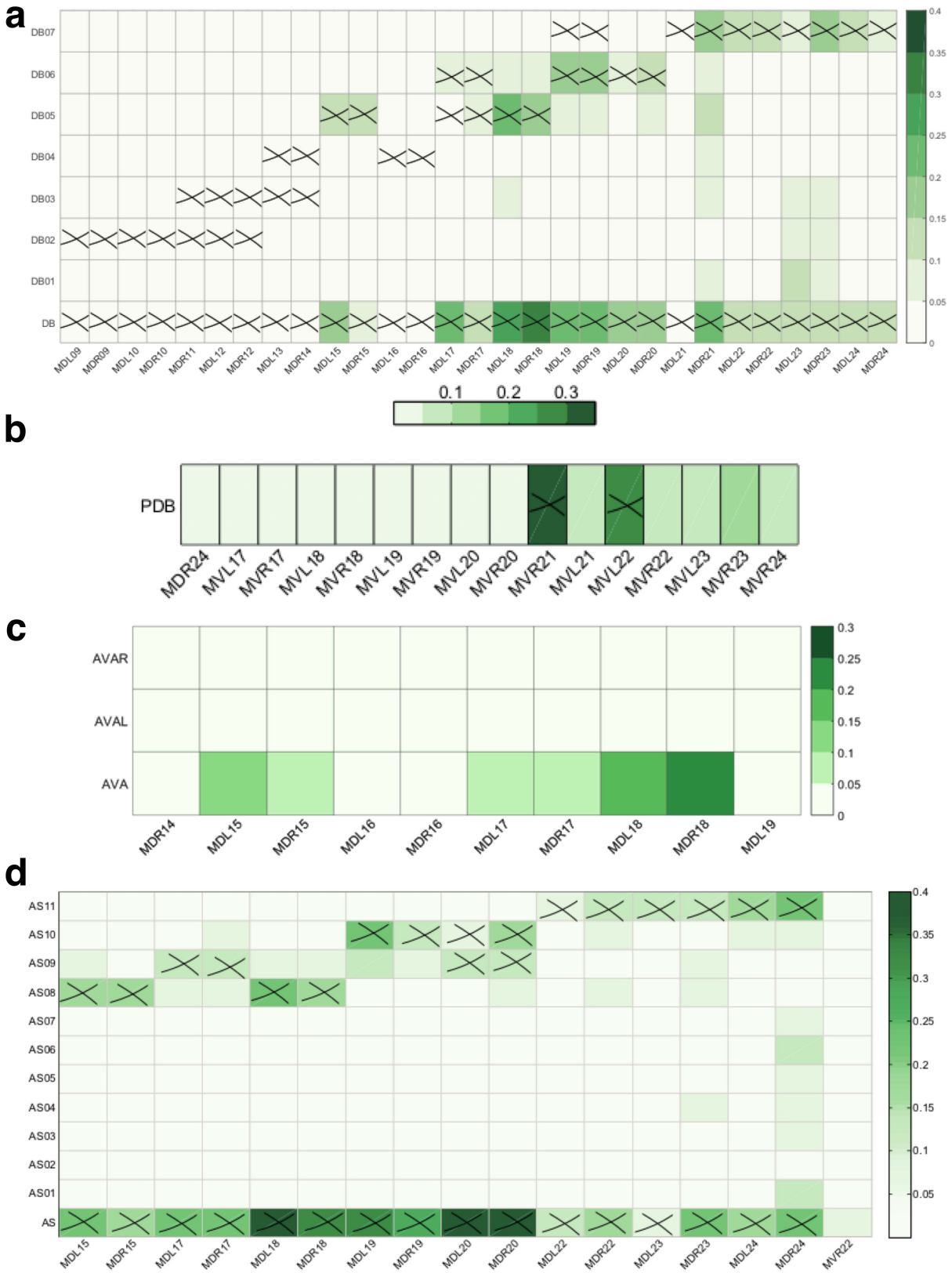

Extended Data Figure 8 | The role of individual neurons within the DB, PDB, AVA, and AS neuronal classes. Role of neurons within the DB (**a**), PDB (**b**), AVA (**c**), and AS (**d**) neuronal classes in the loss of muscular controllability in *C. elegans*. The shade of green represents the probability with which control is lost over each muscle following the ablation of individual neurons. Each cross indicates a direct connection between a neuron and a muscle cell. Note that there are other muscles directly connected to the neurons but not shown here, because of zero probability for reduced control over these muscles following ablation of these neuronal classes.

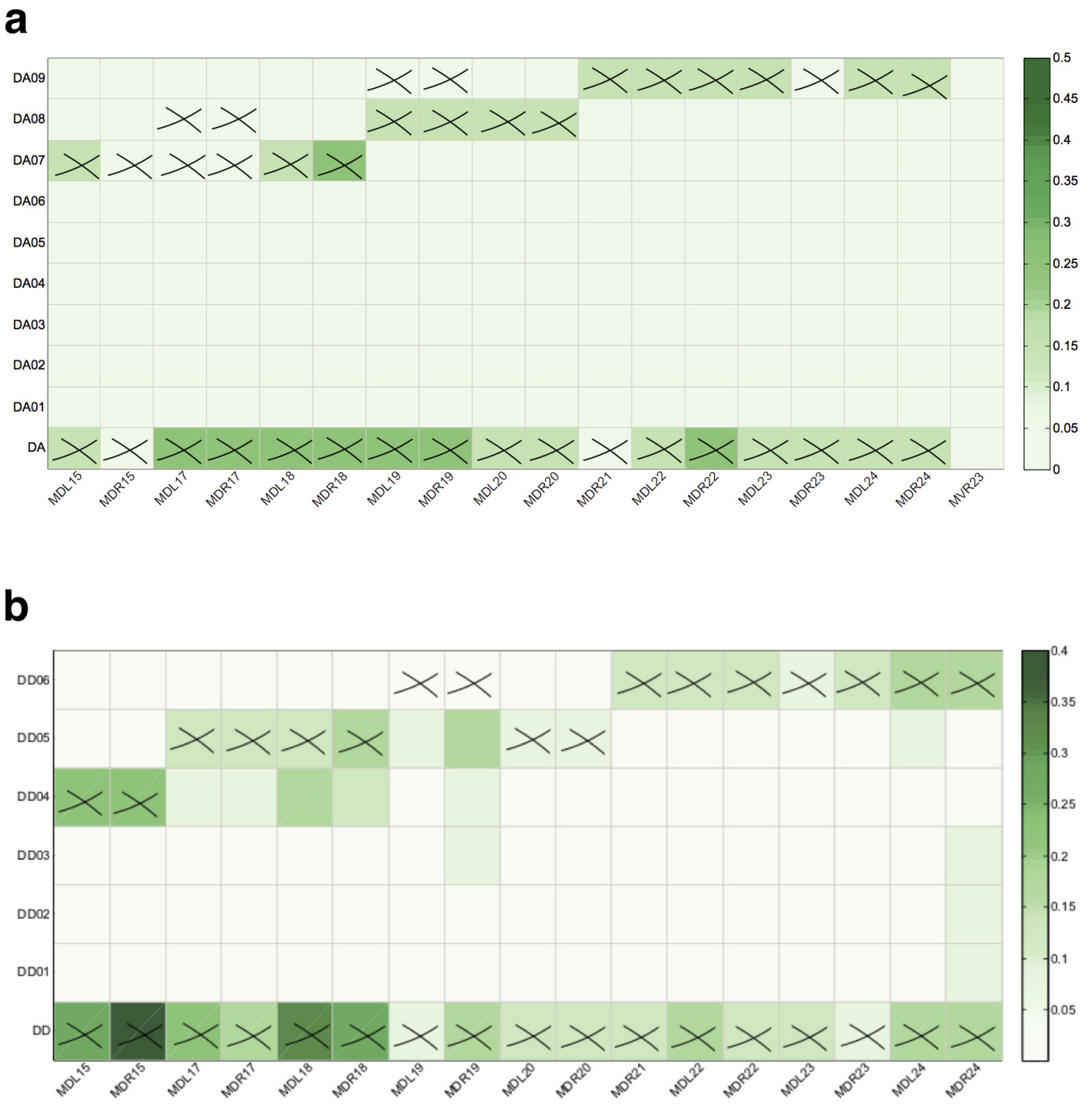

Extended Data Figure 9 | The role of individual neurons within the DA and DD neuronal classes. Role of neurons within the DA (**a**) and DD (**b**) neuronal classes in the loss of muscular controllability in *C. elegans*. The shade of green represents the probability with which the control is lost over each muscle induced by the ablation of individual neurons. Each cross indicates a direct connection between a neuron and a muscle cell. Note that there are other muscles directly connected to the neurons but not shown here, because of zero probability for reduced control over these muscles following ablation of these neuronal classes.

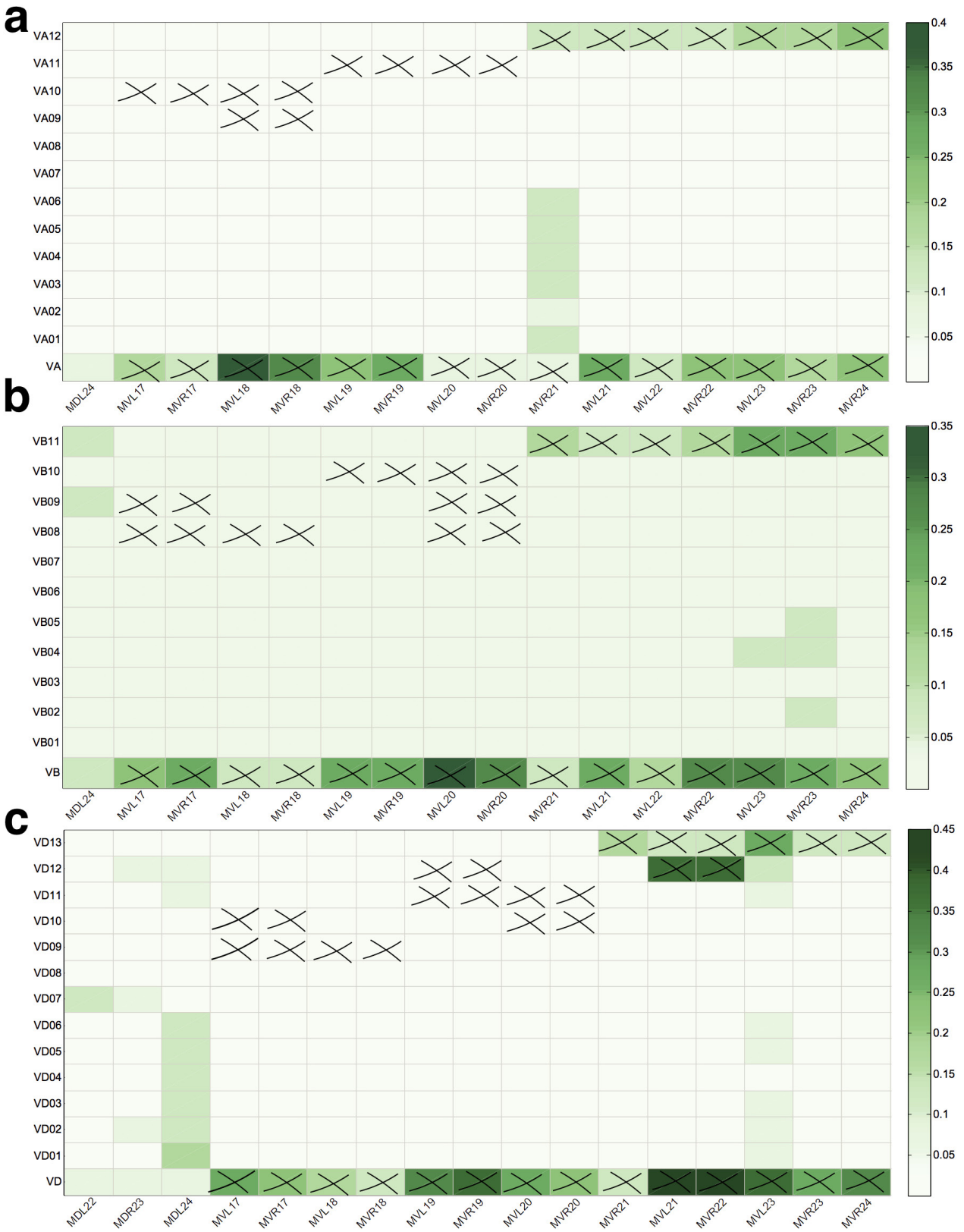

Extended Data Figure 10 | The role of individual neurons within the VA, VB, and VD neuronal classes. Role of neurons within the VA (**a**), VB (**b**) and VD (**c**) neuronal classes in the loss of muscular controllability in *C. elegans*. The shade of green represents the probability with which the control is lost over each muscle induced by the ablation of individual neurons. Each cross indicates a direct connection between a neuron and a muscle cell. Note that there are other muscles directly connected to the neurons but not shown here, because of zero probability for reduced control over these muscles following ablation of these neuronal classes.

nature research

Corresponding Author: Albert-Laszlo Barabasi

Date: Jul 21, 2017

Life Sciences Reporting Summary

Nature Research wishes to improve the reproducibility of the work we publish. This form is published with all life science papers and is intended to promote consistency and transparency in reporting. All life sciences submissions use this form; while some list items might not apply to an individual manuscript, all fields must be completed for clarity.

For further information on the points included in this form, see Reporting Life Sciences Research. For further information on Nature Research policies, including our data availability policy, see Authors & Referees and the Editorial Policy Checklist.

Experimental design

1. Sample size

   Describe how sample size was determined.

   SI, Section IIIB - This sample size was chosen as it was previously shown to provide sufficient phenotyping sampling (Yemini 2013, Nature Methods)

2. Data exclusions

   Describe any data exclusions.

   No animals were excluded from analysis.

3. Replication

   Describe whether the experimental findings were reliably reproduced.

   The method of predicting the function of neurons is deterministic and reliably reproducible; For the laser ablation experimental validations, all attempts at replication were successful.

4. Randomization

   Describe how samples/organisms/participants were allocated into experimental groups.

   SI, Section IIIB

5. Blinding

   Describe whether the investigators were blinded to group allocation during data collection and/or analysis.

   Blinding was unnecessary as all analysis was automated through use of custom software.

Note: all studies involving animals and/or human research participants must disclose whether blinding and randomization were used.

6. Statistical parameters

   For all figures and tables that use statistical methods, confirm that the following items are present in relevant figure legends (or the Methods section if additional space is needed).

n/a	Confirmed	
☐	☒	The exact sample size (*n*) for each experimental group/condition, given as a discrete number and unit of measurement (animals, litters, cultures, etc.)
☐	☒	A description of how samples were collected, noting whether measurements were taken from distinct samples or whether the same sample was measured repeatedly.
☐	☒	A statement indicating how many times each experiment was replicated
☐	☒	The statistical test(s) used and whether they are one- or two-sided (note: only common tests should be described solely by name; more complex techniques should be described in the Methods section)
☒	☐	A description of any assumptions or corrections, such as an adjustment for multiple comparisons
☐	☒	The test results (e.g. *p* values) given as exact values whenever possible and with confidence intervals noted
☐	☒	A summary of the descriptive statistics, including central tendency (e.g. median, mean) and variation (e.g. standard deviation, interquartile range)
☐	☒	Clearly defined error bars

See the web collection on statistics for biologists for further resources and guidance.

Software

Policy information about availability of computer code

7. Software

Describe the software used to analyze the data in this study.	The software of video analyses is Worm Tracker (Yemini 2013, Nature Methods) which is publicly available; The software of statistical analyses is GraphPad Prism (publicly available); The method of theoretical analyses is described in SI Sec. II.

For all studies, we encourage code deposition in a community repository (e.g. GitHub). Authors must make computer code available to editors and reviewers upon request. The *Nature Methods* guidance for providing algorithms and software for publication may be useful for any submission.

Materials and reagents

Policy information about availability of materials

8. Materials availability

Indicate whether there are restrictions on availability of unique materials or if these materials are only available for distribution by a for-profit company.	The C. elegans connectome data is publicly available and the details were described in SI, Sec I.A.

9. Antibodies

Describe the antibodies used and how they were validated for use in the system under study (i.e. assay and species).	NA

10. Eukaryotic cell lines

a. State the source of each eukaryotic cell line used.	NA
b. Describe the method of cell line authentication used.	NA
c. Report whether the cell lines were tested for mycoplasma contamination.	NA
d. If any of the cell lines used in the paper are listed in the database of commonly misidentified cell lines maintained by ICLAC, provide a scientific rationale for their use.	NA

Animals and human research participants

Policy information about studies involving animals; when reporting animal research, follow the ARRIVE guidelines

11. Description of research animals

Provide details on animals and/or animal-derived materials used in the study.	Nematode worms (C. elegans).

Policy information about studies involving human research participants

12. Description of human research participants

Describe the covariate-relevant population characteristics of the human research participants.	NA